A hypoxia-induced Rab pathway regulates embryo implantation by controlled trafficking of secretory granules

Arpita Bhurke[a], Athilakshmi Kannan[a], Alison Neff[b], Qiuyan Ma[b], Mary J. Laws[a], Robert N. Taylor[c], Milan K. Bagchi[b,1], and Indrani C. Bagchi[a,1]

[a]Department of Comparative Biosciences, University of Illinois at Urbana–Champaign, Urbana, IL 61802 [b]Department of Molecular and Integrative Physiology, University of Illinois at Urbana–Champaign, Urbana, IL 61801 and [c]Department of Obstetrics and Gynecology, University of Utah School of Medicine, Salt Lake City, UT 84132

Implantation is initiated when an embryo attaches to the uterine luminal epithelium and subsequently penetrates into the underlying stroma to firmly embed in the endometrium. These events are followed by the formation of an extensive vascular network in the stroma that supports embryonic growth and ensures successful implantation. Interestingly, in many mammalian species, these processes of early pregnancy occur in a hypoxic environment. However, the mechanisms underlying maternal adaptation to hypoxia during early pregnancy remain unclear. In this study, using a knockout mouse model, we show that the transcription factor hypoxia-inducible factor 2 alpha (Hif2α), which is induced in subluminal stromal cells at the time of implantation, plays a crucial role during early pregnancy. Indeed, when preimplantation endometrial stromal cells are exposed to hypoxic conditions in vitro, we observed a striking enhancement in HIF2α expression. Further studies revealed that HIF2α regulates the expression of several metabolic and protein trafficking factors, including RAB27B, at the onset of implantation. RAB27B is a member of the Rab family of GTPases that allows controlled release of secretory granules. These granules are involved in trafficking MMP-9 from the stroma to the epithelium to promote luminal epithelial remodeling during embryo invasion. As pregnancy progresses, the HIF2α-RAB27B pathway additionally mediates crosstalk between stromal and endothelial cells via VEGF granules, developing the vascular network critical for establishing pregnancy. Collectively, our study provides insights into the intercellular communication mechanisms that operate during adaptation to hypoxia, which is essential for embryo implantation and establishment of pregnancy.

endometrium | implantation | hypoxia | granules | RAB

Implantation in the mouse and human is initiated when the blastocyst trophectoderm attaches to the uterine luminal epithelium and subsequently penetrates the underlying stroma to firmly embed in the maternal endometrium. This is followed by formation of an extensive vascular network in the decidua that supports the growing embryo before placentation (1–6). Failure of any of these processes to proceed normally can result in a number of diseases of pregnancy such as recurrent miscarriage, preeclampsia, and intrauterine growth restriction (7–9). A current challenge is to understand the complex processes by which intercellular communications between epithelial–stromal and stromal–endothelial cells of the endometrium occur to ensure successful implantation and establishment of pregnancy.

Many aspects of implantation remain unclear, but there is little doubt that concerted actions of the ovarian steroid hormones progesterone (P) and 17β-estradiol (E) in the uterine cells are essential for embryo implantation and establishment of pregnancy (1, 4, 10–12). In the past decade, several steroid-regulated transcription factors have been described that control implantation (2, 3, 5, 12). Less clear are the precise mechanisms by which paracrine signals generated downstream of these factors are transmitted from one uterine cell compartment to another to create a tissue functionally competent for blastocyst implantation and establishment of pregnancy.

In this study, we report that E markedly induces expression of HIF2α in P-primed endometrial stromal cells at the onset of implantation. HIF2α, is a member of the family of hypoxia-inducible transcription factors (HIFs) that critically regulate a tissue's response to changes in oxygen levels (13). While HIF1α expression in the uterus does not change during early pregnancy, HIF2α is induced selectively in the subluminal stromal cells (14). This finding is of great interest, because it has long been known that the maternal environment during implantation is hypoxic (15, 16). However, the mechanisms that enable maternal adaptation to hypoxia during this process remain unclear. Using genetic, molecular, and cell biological approaches, this study demonstrates that uterine stromal HIF2α regulates the trafficking of MMP-9 secretory granules, which mediate stromal–epithelial crosstalk to promote epithelial remodeling and permit implantation. As pregnancy progresses, hypoxia-induced trafficking of VEGF granules between stromal and endothelial cells promotes development of the vascular network critical for successful perfusion of the growing pregnancy. Together, the findings of this study provide important insights into the molecular basis of adaptation to hypoxia, which is critical for embryo implantation and establishment of pregnancy.

Significance

In many mammalian species, embryo implantation and processes of early pregnancy occur in a hypoxic environment. However, the mechanisms underlying maternal adaptation to hypoxia during early pregnancy remain unclear. This work has uncovered an important mechanism in mammalian reproduction and development by identifying maternal secretory granules that mediate molecular dialogue between the maternal tissue compartments during early pregnancy. This dialogue, which is the molecular basis of adaptation to hypoxia, is critical for embryo implantation and establishment of pregnancy.

www.manaraa.com

Results

In mice, implantation is initiated 4 d after fertilization, when the blastocyst reaches the uterus (14). Previous studies indicated that HIF1α expression in the uterus does not change during implantation, but HIF2α is induced selectively in the subluminal stromal cells (14). To analyze hormonal regulation of induction of HIF2α during implantation, we utilized a delayed implantation model (17–19). Removal of the ovaries several hours before implantation blocks implantation due to the lack of ovarian steroids. Continued administration of P alone to these ovariectomized pregnant animals allows blastocysts to remain viable, but attachment of the embryo to the uterine epithelium does not occur in the absence of E. Administration of E to the P-primed mice promotes attachment of the blastocyst trophectoderm to the luminal epithelium within 24 h.

Immunofluorescence (IF) analysis showed that the HIF2α protein, which was barely detectable in uterine sections of P-supplemented delayed animals prior to E administration (Fig. 1 *A*, *Left*), was dramatically induced selectively in endometrial stromal cells subjacent to the luminal epithelium within 24 h of E treatment (Fig. 1 *A*, *Right*). No expression of HIF2α protein was detected in luminal epithelium. These results identified HIF2α as an E-regulated factor in P-primed endometrium during implantation. Consistent with this observation, when preimplantation endometrial stromal cells on day 4 of pregnancy were exposed to hypoxic conditions in vitro, we observed a striking enhancement in HIF2α expression (Fig. 1*B*).

To investigate the function of HIF2α in the uterus, we created a conditional knockout of this gene in adult uterine tissue. Crossing mice that harbor the "floxed" *Hif2α* gene (*Hif2α*$^{f/f}$) with progesterone receptor (PR)-Cre mice generated *Hif2α*$^{d/d}$ mice. As shown in Fig. 1*C*, prominent HIF2α expression was observed in uterine stromal cells of *Hif2α*$^{f/f}$ mice on day 5 of normal pregnancy. By contrast, HIF2α expression was not detectable but HIF1α expression was unaffected in uterine sections from *Hif2α*$^{d/d}$ mice, indicating successful abrogation of the *Hif2α* gene in uterine

stromal cells (Fig. 1*C*). Since PR-Cre is not expressed in the germ cells and therefore does not excise the floxed allele in these cells, the floxed *Hif2α* gene remains intact in embryos resulting from crossing of PR-Cre females with wild-type males. HIF2α expression is observed in the blastocysts isolated from pregnant *Hif2α*$^{f/f}$ females and also in blastocysts present in vivo at the implantation sites of these females (*SI Appendix*, Fig. S1). As explained above, the *Hif2α* conditional allele remains intact in embryos present in pregnant *Hif2α*$^{d/d}$ females and therefore the embryos collected from these females, or present at the implantation sites, exhibit HIF2α expression. While HIF2α expression is lost in the endometrial stromal cells of *Hif2α*$^{d/d}$ females, it remains intact in the blastocysts present in *Hif2α*$^{d/d}$ females (*SI Appendix*, Fig. S1).

A 6-mo breeding study using wild-type males demonstrated that *Hif2α*$^{d/d}$ females had no offspring (*SI Appendix*, Fig. S2A). The number of blastocysts recovered from *Hif2α*$^{f/f}$ and *Hif2α*$^{d/d}$ uteri and the serum levels of P and E were comparable on day 4 of pregnancy, indicating normal ovarian function, fertilization, and embryo transport in the two genotypes (*SI Appendix*, Fig. S2 *B–D*).

We next examined embryo implantation in *Hif2α*$^{f/f}$ and *Hif2α*$^{d/d}$ females by employing the blue dye assay (20, 21), which assesses increased vascular permeability at implantation sites. The blue bands are the first discernible signs of impending implantation. Both *Hif2α*$^{f/f}$ and *Hif2α*$^{d/d}$ uteri displayed distinct blue bands (*SI Appendix*, Fig. S3, *Upper*), indicating implantation sites on the morning of day 5 of pregnancy. Statistical analysis revealed no difference between the number of implantation sites in *Hif2α*$^{f/f}$ and *Hif2α*$^{d/d}$ females (*SI Appendix*, Fig. S3, *Lower*). While previous reports implicated HIF1α in regulation of uterine vascular permeability (22), our results indicated that HIF2α is not involved in this process.

Histological analysis of *Hif2α*$^{f/f}$ and *Hif2α*$^{d/d}$ females on the morning of day 5 of pregnancy revealed close contact of embryonic trophectoderm with uterine luminal epithelium, indicating that embryo attachment had occurred (Fig. 2*A*). When examined 12 h later, on the evening of day 5, the implanting blastocyst in *Hif2α*$^{f/f}$ females had breached the luminal epithelium
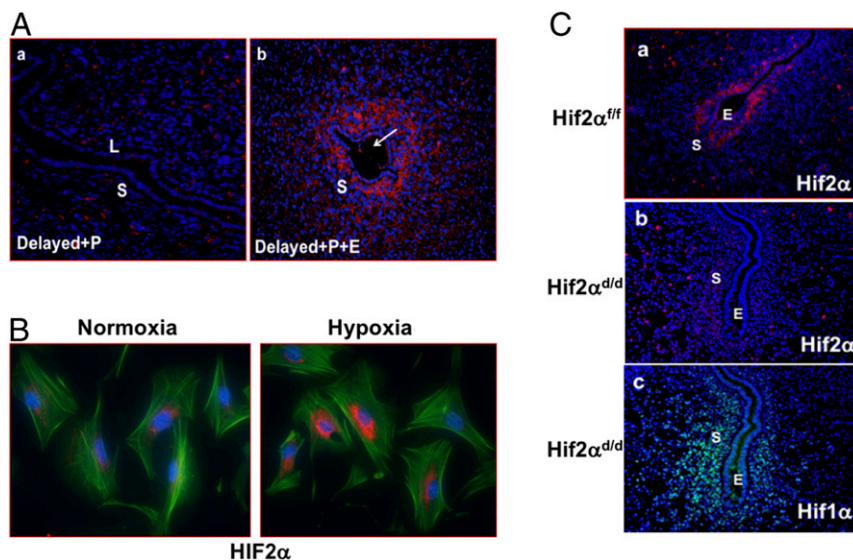
Fig. 1. (*A*) Induction of HIF2α expression in uterine stromal cells during delayed implantation. Uterine sections from delayed mice treated with P (*A*) and P plus E (*B*) for 24 h. The sections were subjected to IF using HIF2α antibody. L and S indicate luminal epithelium and stroma. Embryo is indicated by an arrowhead. Data were repeated with n = 3 mice. Representative images are shown. (*B*) Induction of HIF2α in preimplantation stromal cells exposed to hypoxic conditions. Mouse endometrial stromal cells isolated from uteri on day 4 of pregnancy were cultured under normoxic (*Left*) and hypoxic (3%) (*Right*) conditions for 48 h, fixed, and subjected to IF using HIF2α antibody. Data were repeated with n = 3 mice. Representative images are shown. (*C*) Efficient ablation of HIF2α in the uterus during implantation. Uterine sections obtained from day 5 pregnant *Hif2α*$^{f/f}$ (a) and *Hif2α*$^{d/d}$ (b) mice were subjected to IF using anti-HIF2α antibody. Note the lack of HIF2α immunostaining in uteri of the mutant mice. HIF1α expression was unaffected in the uteri of mutant mice (c). S and E indicate stroma and embryo. Blue: DAPI. Data were repeated with n = 2 mice. Representative images are shown.

Bhurke et al.

to firmly embed itself in the maternal stroma (Fig. 2 *B, a*). By contrast, blastocysts in *Hif2α^{d/d}* females failed to penetrate the epithelium and remained within the uterine lumen (Fig. 2 *B, b*). Cytokeratin immunostaining of uterine epithelial cells the evening of day 5 of pregnancy indicated that in *Hif2α^{f/f}* uteri, the breached luminal epithelium was degraded; in *Hif2α^{d/d}* uteri, it remained intact with no signs of penetration by the blastocyst (Fig. 2 *C, a* and *b*).

Endometrial structural remodeling that results in loss of integrity of luminal epithelium, facilitating embryo implantation, encompasses two critical molecular processes: remodeling of the epithelial–stromal basement membrane and disruption of the epithelial cell–cell junctions (23–25). Analysis of uterine sections with Jones' stain—a methenamine silver-periodic acid-Schiff stain used to delineate basement membrane—indicates degradation of the basement membrane at the site of embryo invasion in *Hif2α^{f/f}* mice. Such basement membrane degradation fails to occur in the *Hif2α^{d/d}* mice (Fig. 2 *D, Upper*). Following basement membrane remodeling in *Hif2α^{f/f}* mice, the epithelial junctions are disrupted. The disappearance of epithelial (E)-cadherin, a component of the intercellular adherent junctions in the uterine luminal epithelium, is a hallmark of successful epithelial remodeling that allows implantation. We observed sharp downregulation of E-cadherin in the epithelium of *Hif2α^{f/f}* uteri on day 5 of gestation, whereas E-cadherin expression remained intact in adherens junctions of *Hif2α^{d/d}* uteri (Fig. 2 *D, Lower*). Collectively, these results indicate that, in the absence of maternal HIF2α, the luminal epithelium does not undergo the remodeling that allows an embryo to breach and embed in the stroma, leading to failure of implantation. It is important to note that the *Hif2α* allele is intact in the embryos resulting from crosses of *Hif2α^{d/d}* females with wild-type males. Thus, the observed failure of implantation in *Hif2α^{d/d}* mice is due not to an intrinsic lack of this gene in the embryo but rather to a deficiency of HIF2α in the maternal tissue.

It is widely accepted that basement membrane remodeling is mediated by MMPs, a family of zinc-dependent endopeptidases that cleave structural elements of the extracellular matrix (ECM) and also process a variety of non-ECM substrates (26–32). Some MMPs, including *Mmp-9* and *Mmp-2*, are reportedly expressed in stromal cells at the implantation site, raising the possibility that these factors, when secreted, may act on the epithelial cells in a paracrine manner to influence basement membrane remodeling and junctional disruption (28, 30, 31). Interestingly, previous studies have shown that HIFs in certain cells, such as chondrocytes, regulate the expression of *Mmp-9* (33). This led us to examine whether MMP-9 expression is regulated by HIF2α in endometrial stromal cells. Immunohistochemical analysis of uterine sections from *Hif2α^{f/f}* and *Hif2α^{d/d}* on day 5 of pregnancy revealed comparable levels of MMP-9 expression in the two genotypes (*SI Appendix,* Fig. S4), indicating that HIF2α does not directly control *Mmp-9* gene expression. However, when we cultured stromal cells from *Hif2α^{f/f}* and *Hif2α^{d/d}* uteri and monitored MMP-9 expression, we observed distinctly different localizations of MMP-9 in the two genotypes. In control stromal
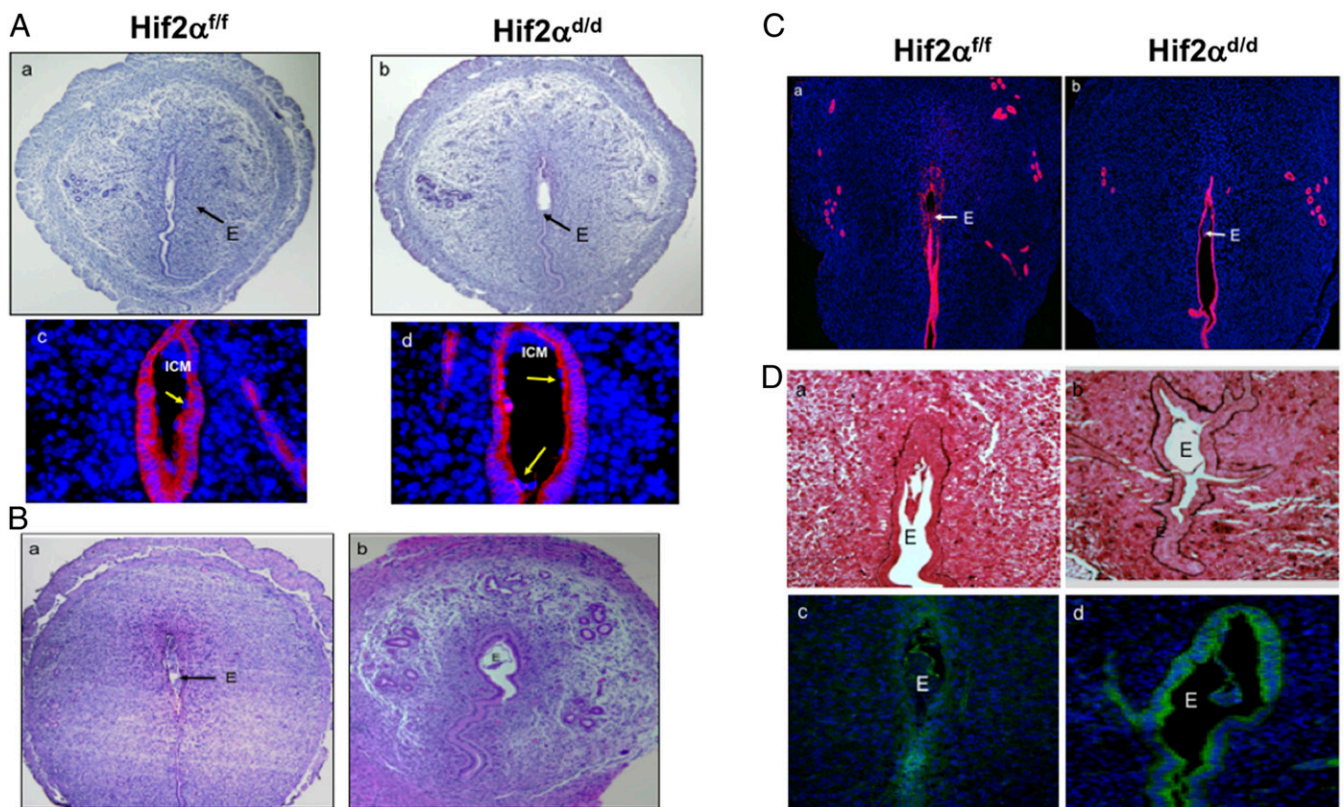

Fig. 2. The embryo fails to invade through the luminal epithelium in *Hif2α^{d/d}* mice. (*A, Upper*) H&E staining of uterine sections obtained from *Hif2α^{f/f}* (*a*) and *Hif2α^{d/d}* (*b*) mice (*n* = 5) on the morning of day 5 of pregnancy. Black arrows indicate embryo. (*A, Lower*) Implantation sites from *Hif2α^{f/f}* (*Left*) and *Hif2α^{d/d}* (*Right*) mice on the morning of day 5 were subjected to IF using anti-cytokeratin antibody (red). Yellow arrows indicate trophoblast cells of the embryo. (*B*) H&E staining of uterine sections obtained from *Hif2α^{f/f}* (*a*) and *Hif2α^{d/d}* (*b*) mice (*n* = 6) on the evening of day 5 of pregnancy. E represents embryo. (*C*) Uterine sections obtained from day 5 pregnant *Hif2α^{f/f}* (*a*) and *Hif2α^{d/d}* (*b*) mice were subjected to IF using anti-cytokeratin antibody. *n* = 5 embryos were examined per animal. (*D, Upper*) Uterine sections from *Hif2α^{f/f}* (*a*) and *Hif2α^{d/d}* (*b*) mice on day 5 were subjected to Jones' silver staining. The basement membrane (black) is observed at the base of the luminal epithelium. E represents embryo. (*D, Lower*) Uterine sections from *Hif2α^{f/f}* (*c*) and *Hif2α^{d/d}* (*d*) mice on the evening of day 5 were subjected to IF using anti-E-cadherin antibody. *n* = 5 embryos were examined per animal.

Bhurke et al.

www.manaraa.com

cells from $Hif2\alpha^{f/f}$ uteri, MMP-9 was localized predominantly at the plasma membrane; but in stromal cells from $Hif2\alpha^{d/d}$ uteri, MMP-9 expression appeared to be sequestered in the perinuclear Golgi (Fig. 3A). Consistent with these observations was the marked decline in levels of MMP-9, but not of MMP-2, noted in the conditioned media of cultured stromal cells from $Hif2\alpha^{d/d}$ uteri compared to $Hif2\alpha^{f/f}$ controls (Fig. 3B). These results indicated that HIF2α specifically regulates secretion of MMP-9 in endometrial stromal cells.

To investigate the molecular basis of the secretory defect in uteri lacking HIF2α, we isolated mouse endometrial stromal cells (MESCs) from $Hif2\alpha^{f/f}$ and $Hif2\alpha^{d/d}$ uteri on day 5 of pregnancy and performed gene expression profiling. Interestingly, our study revealed a marked decline in the levels of transcript corresponding to $Rab27b$ in stromal cells of $Hif2\alpha^{d/d}$ uteri (Fig. 4 A, Upper Left). The expression of $Rab27a$, a close member of this family of proteins, remained unaltered in stromal cells of $Hif2\alpha^{d/d}$ uteri (Fig. 4 A, Upper Right). Consistent with the RNA profile, we observed robust expression of RAB27B protein in stromal cells surrounding the implanted embryo of $Hif2\alpha^{f/f}$ uteri, whereas its expression was dramatically down-regulated in $Hif2\alpha^{d/d}$ uterine stromal cells on day 5 of gestation (Fig. 4 A, Lower). Immunocytochemistry of $Hif2\alpha^{f/f}$ endometrial stromal cells showed that RAB27B and MMP-9 are both present at the cell membrane of these cells with significant colocalization, whereas such localization of these proteins was not found in stromal cells from $Hif2\alpha^{d/d}$ uteri (Fig. 4B). These results indicated that HIF2α regulates RAB27B

expression, which then mediates MMP-9 trafficking to the plasma membrane of endometrial stromal cells.

We next investigated whether $Rab27b$ is a direct target of HIF2α in endometrial stromal cells. Bioinformatic analyses revealed the presence of two sites resembling the consensus hypoxia-response element (HRE) in the $Rab27b$ gene. We performed chromatin immunoprecipitation (ChIP) analysis to determine the enrichment of HIF2α at these sites in uterine stromal cells cultured under normoxic and hypoxic conditions. We observed minimal occupancy of HIF2α at the −84.8 site of the $Rab27b$ gene as well as a negative control region under both conditions. In contrast, a marked enhancement of HIF2α occupancy was observed at the +58.4 kb HRE in response to hypoxia (Fig. 4C). These results indicate that hypoxia-induced accumulation of HIF2α triggers its binding to the HRE of the $Rab27b$ gene to regulate its expression in endometrial stromal cells.

Since previous reports implicated RAB27B in regulated release of secretory granules in certain cells including platelet dense granules and pancreatic acinar granules (34, 35), we next investigated whether the Hif2α-Rab27b pathway regulates subcellular distribution of secretory granules in endometrial stromal cells during pregnancy. Stromal cells isolated from uteri on day 4 of pregnancy were subjected to immunocytochemical staining using antibody against CD63, a glycoprotein of the tetraspanin family. Intracellular CD63 trafficking is associated with granule-derived secretory pathways (36, 37). Our studies revealed that the CD63-positive granules were distributed diffusely throughout
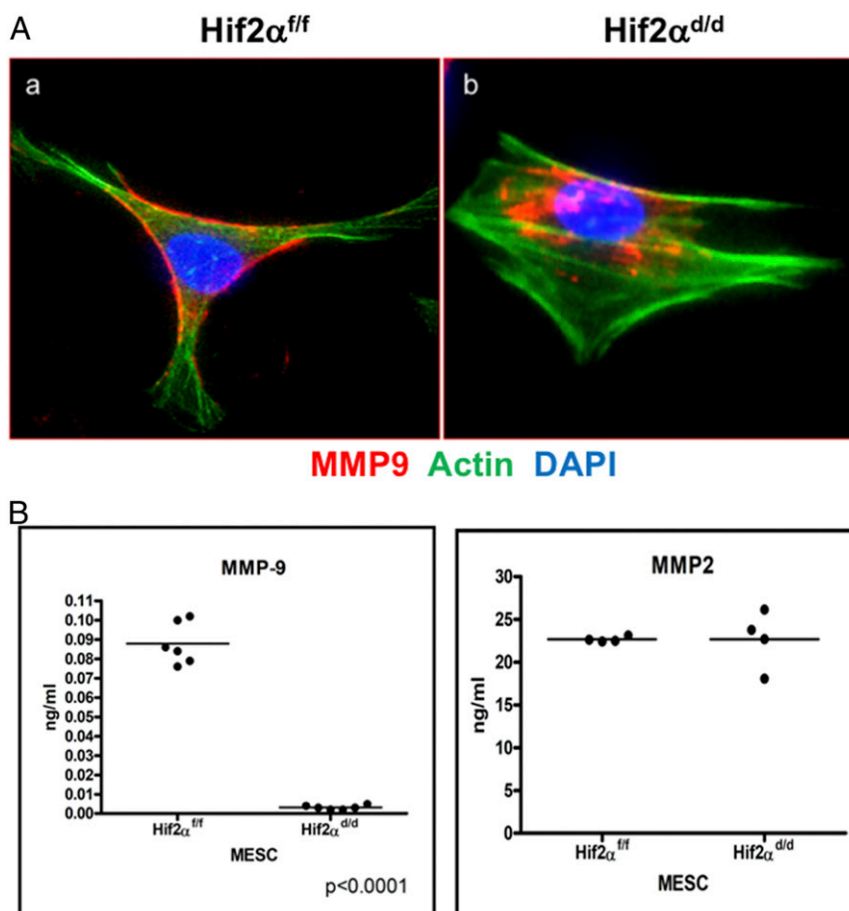
Fig. 3. HIF2α regulates MMP-9 secretion of mouse endometrial stromal cells. (A) Mouse endometrial stromal cells isolated from $Hif2\alpha^{f/f}$ (a) and $Hif2\alpha^{d/d}$ (b) uteri on day 4 of pregnancy were cultured for 48 h, fixed, and subjected to IF using MMP-9 antibody. Data were repeated with $n = 3$ mice and for each sample 35 to 50 cells were examined over multiple fields. Representative images are shown. (B) Conditioned media from cultured stromal cells isolated from $Hif2\alpha^{f/f}$ and $Hif2\alpha^{d/d}$ uteri were analyzed for MMP-9 (Left) and MMP-2 (Right) using ELISA. Data represent mean ± SEM from three separate samples.
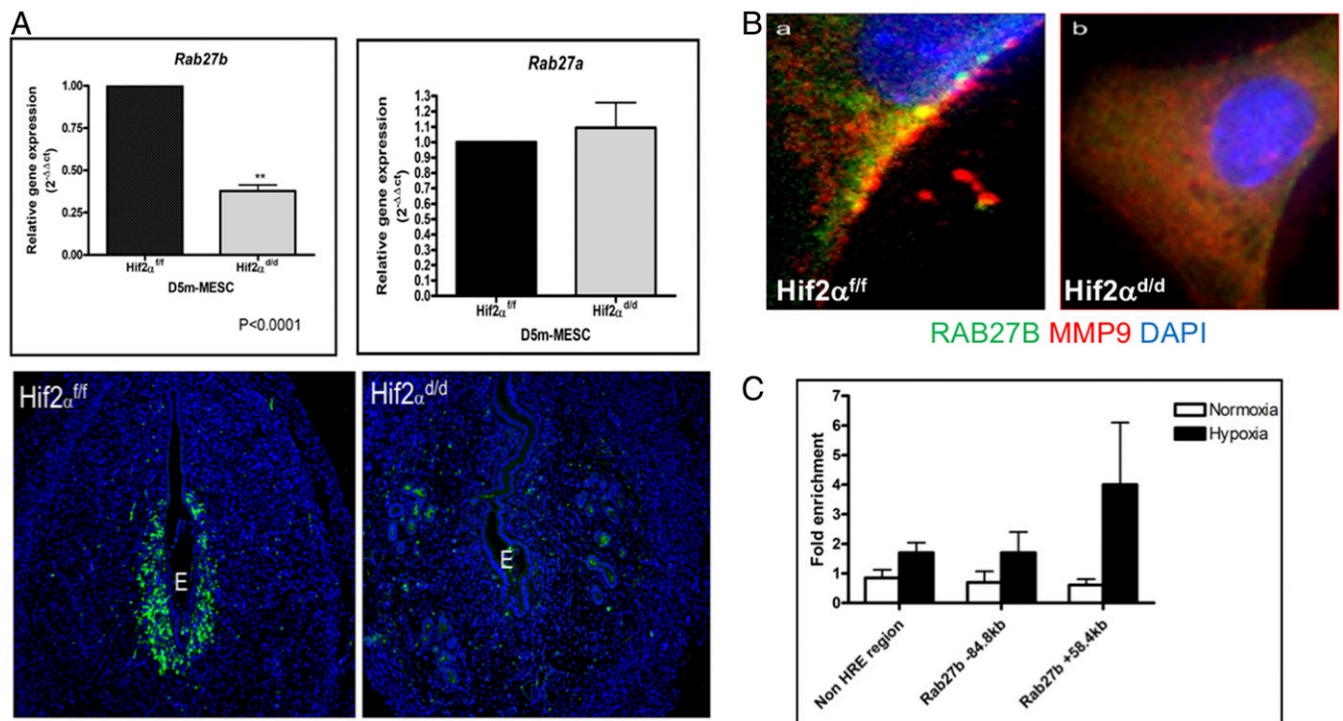
Bhurke et al.

Fig. 4. HIF2α induces RAB27B expression in uterine stromal cells during implantation. (*A Upper*) qPCR analysis of Rab27a and Rab27b mRNAs in *Hif2α^f/f^* and *Hif2α^d/d^* uterine stromal cells. (*A, Lower*) IF analysis of RAB27B (green) in *Hif2α^f/f^* and *Hif2α^d/d^* uteri on day 5 of pregnancy. *n* = 3 mice were examined. (*B*) IF analysis of RAB27B (green) and MMP-9 (red) in *Hif2α^f/f^* and *Hif2α^d/d^* uteri on day 5 of pregnancy. Note colocalization of RAB27B and MMP-9 (yellow) in MESCs. Data were repeated with *n* = 3 mice and for each sample 35 to 50 cells were examined over multiple fields. Representative images are shown. (*C*) Mouse stromal cells were cultured under normoxic or hypoxic conditions. Chromatin immunoprecipitation was performed using HIF2α antibody, as described in *Materials and Methods*. Chromatin enrichment was quantified by real-time PCR using primers flanking the potential HRE in the *Rab27b* promoter and also a negative control region in the non-HRE region of *Rab27b*. Enrichments were normalized to 1% of input DNA. The experiment was repeated twice; representative data are shown.

the *Hif2α^f/f^* stromal cells (Fig. 5 *A, Left*). In contrast, *Hif2α^d/d^* stromal cells exhibited perinuclear accumulation of CD63-positive granules (Fig. 5 *A, Right*). To determine the role of Rab27b in trafficking of CD63-positive granules, we next used RNA interference to silence endogenous *Rab27b* expression in endometrial stromal cells. MESCs were transfected with siRNA targeted specifically to the mRNA of *Rab27b*. Cells in control experiments were transfected with a scrambled siRNA. Endometrial stromal cells treated with siRNA targeted to *Rab27b* mRNA efficiently suppressed the level of its cognate mRNA but did not significantly affect the level of *Rab27a*, *Hif2α*, or *Mmp-9* mRNAs (*SI Appendix,* Fig. S5). This down-regulation of *Rab27b* expression in MESCs was associated with perinuclear accumulation of secretory granules (Fig. 5 *B, Lower*). In MESCs transfected with control siRNA, CD63-positive secretory granules were aligned with actin filaments and localized predominantly near the periphery of stromal cells (Fig. 5 *B, Upper*). Consistent with these observations, we noted MMP-9 accumulation close to the nucleus in stromal cells transfected with *Rab27b* siRNAs (Fig. 5 *C, Right*). By contrast, in MESCs transfected with control siRNA, MMP-9 is clearly localized to the cell membrane (Fig. 5 *C, Left*). Consequently, we saw a marked decline in MMP-9 levels in the conditioned media of cultured stromal cells transfected with *Rab27b* siRNAs, compared to cells treated with control siRNAs (Fig. 5 *D, Left*). MMP-2 levels in the conditioned media were similar in cultured stromal cells transfected with *Rab27b* siRNAs or with control siRNAs (Fig. 5 *D, Right*). Taken together, these results strongly suggest that CD63-positive secretory granules associated with RAB27B are involved in MMP-9 trafficking in endometrial stromal cells.

To further address the contribution of Hif2α-mediated secretion of MMP-9 in epithelial remodeling, we performed in vitro experiments employing Ishikawa endometrial epithelial cells. We observed that Ishikawa cells grown to near confluency exhibited prominent junctional E-cadherin staining, indicating formation of adherent junctions by these cells (Fig. 5 *E, Upper Left*). When these cells were treated with recombinant MMP-9, the staining of E-cadherin was drastically reduced, indicating a disruption in cellular adherent junctions (Fig. 5 *E, Upper Right*). This result provided direct evidence that MMP-9 is able to induce epithelial remodeling.

To confirm that the stromal cell secretions, which include MMP-9, is responsible for epithelial remodeling, conditioned media collected from *Hif2α^f/f^* and *Hif2α^d/d^* stromal cells were added to Ishikawa cells. As shown in Fig. 5 *E, Lower*, when Ishikawa cells were treated with the conditioned media collected from *Hif2α^f/f^* stromal cells, which contains secreted MMP-9, a down-regulation of E-cadherin staining was evident. In contrast, when these cells were treated with the conditioned media collected from *Hif2α^d/d^* stromal cells, which do not secrete MMP-9, epithelial remodeling did not occur as indicated by intact junctional E-cadherin staining. Collectively, these results are consistent with our hypothesis that MMP-9, secreted by the endometrial stromal cells, act on epithelial cells in a paracrine fashion to induce epithelial remodeling.

Embryo invasion into uterine stroma is generally followed by differentiation of stromal cells into decidual cells. Assessment of the decidual response by alkaline phosphate activity (38–41), a known biomarker of decidualization, detected no significant difference between *Hif2α^f/f^* and *Hif2α^d/d^* uteri (*SI Appendix,* Fig.
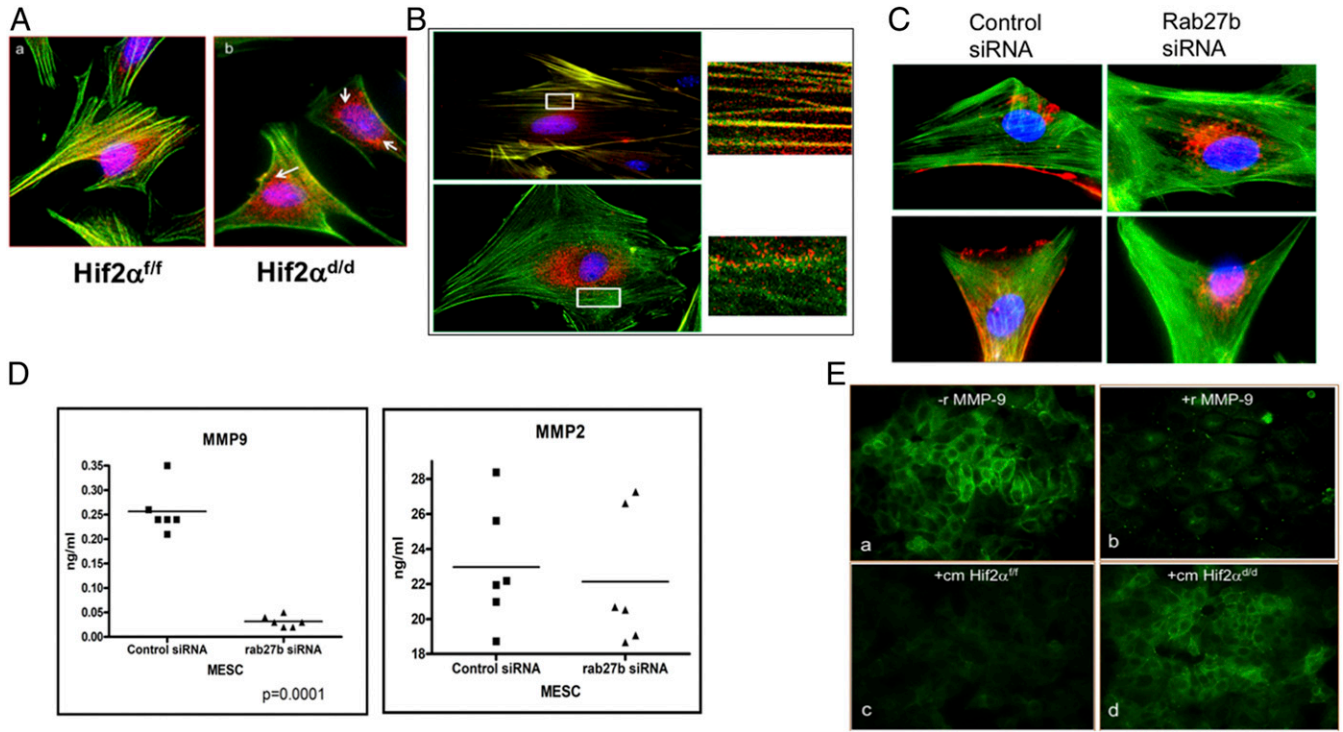
Fig. 5. HIF2α regulates granular secretion in MESCs by controlling Rab27b. (*A*) Mouse endometrial stromal cells isolated from $Hif2\alpha^{f/f}$ (*a*) and $Hif2\alpha^{d/d}$ (*b*) uteri on day 4 of pregnancy were cultured for 48 h, fixed, and subjected to IF using CD63 (red) antibody. Data were repeated with $n = 4$ mice and for each sample 35 to 50 cells were examined over multiple fields. (*B*) MESCs transfected with a scrambled siRNA (*Upper*) and *Rab27b*-specific siRNA (*Lower*) were fixed and subjected to IF using CD63 (red) antibody. Data were repeated with $n = 3$ mice and for each sample 35 to 50 cells were examined over multiple fields. (*C*) MESCs transfected with a scrambled siRNA (*Left*) and *Rab27b*-specific siRNA (*Right*) were fixed and subjected to IF using MMP-9 (red) antibody. Data were repeated with $n = 3$ mice and for each sample 35 to 50 cells were examined over multiple fields. (*D*) Conditioned media (cm) from MESCs transfected with a scrambled siRNA and *Rab27b*-specific siRNA were analyzed for MMP-9 (*Left*) and MMP-2 (*Right*) using ELISA. Data represent mean ± SEM from three separate samples. (*E*) Ishikawa endometrial cells were grown in Dulbecco's modified Eagle medium to ~70% confluence. Cells were then treated with vehicle control (−rMMP9), recombinant MMP-9, 0.001 μg/mL (+rMMP9), conditioned media from MESCs isolated from $Hif2\alpha^{f/f}$ (+cm $Hif2\alpha^{f/f}$) and $Hif2\alpha^{d/d}$ (+cm $Hif2\alpha^{d/d}$) uteri. At 24 h after treatment, cell surface distribution of E-cadherin was examined by immunofluorescence using E-cadherin antibody. The experiments were repeated three times.

S6, *Upper*). We also examined the expression of a panel of factors: *Pgr*, *Hand2*, *Wnt4*, and *CEBPβ*, which are known regulators of decidualization in mice (41–44). Our studies showed a trend that the expression of *Pgr*, *Hand2*, *Wnt4*, and *CEBPβ* mRNAs decrease slightly upon the loss of uterine *Hif2α*, although the differences were not statistically significant. These results indicated that at least certain aspects of the decidualization process progress normally in $Hif2\alpha^{d/d}$ uteri (*SI Appendix*, Fig. S6, *Lower*).

Differentiation of endometrial stromal cells into decidual cells is accompanied by development of vascular networks in the stroma during early pregnancy. We therefore examined the extent of angiogenesis in pregnant uteri of $Hif2\alpha^{d/d}$ mice, employing immunofluorescence using an antibody against platelet/endothelial cell adhesion molecule 1 (PECAM1), a marker of endothelial cells. Uterine sections of the control $Hif2\alpha^{f/f}$ mice on day 6 of pregnancy exhibited a well-developed vascular network spread throughout the decidual bed surrounding the implanted embryo (Fig. 6 *A*, *Upper Left*). By contrast, PECAM1 immunostaining was markedly reduced in uterine sections of pregnant $Hif2\alpha^{d/d}$ mice (Fig. 6 *A*, *Upper Right*). This defect in uterine angiogenesis was also evident in $Hif2\alpha^{f/f}$ and $Hif2\alpha^{d/d}$ uteri subjected to experimentally induced decidualization, indicating impaired development of uterine vasculature in the absence of Hif2α signaling (Fig. 6 *A*, *Lower*).

To gain insight into the angiogenesis defect in the absence of Hif2α signaling, we next examined the expression of PECAM1 and RAB27 in the pregnant uterus. We noted partially overlapping expression patterns of RAB27 and PECAM1 on day 8 of pregnancy (Fig. 6 *B*, *Left*). A subset of stromal cells exhibiting RAB27 immunostaining appeared next to endothelial cells marked by PECAM1, indicating close proximity of stromal cells containing secretory granules to the endothelial network in the decidual bed (Fig. 6 *B*, *Right*). This led us to postulate that stromal cells in which the RAB27B pathway is activated regulate vesicular trafficking of angiogenic factors, such as VEGF, to promote angiogenesis. To test this possibility, we used the RNA-interference technique to silence endogenous *Rab27b* expression in endometrial stromal cells. As shown in Fig. 6C, VEGF expression in stromal cells transfected with control siRNA was distributed throughout the cell extending to the periphery. However, down-regulation of *Rab27b* expression by transfection with *Rab27b* siRNA in stromal cells led to VEGF accumulation near the nucleus (Fig. 6 *C*, *Right*). Further, a significant decline in the levels of VEGFA was noted in the conditioned media of cultured stromal cells transfected with *Rab27b* siRNAs, compared to cells treated with control siRNAs (Fig. 6D).

We next assessed whether HIF2α-RAB27B-mediated vesicular trafficking operates in human endometrial stromal cells. Undifferentiated human endometrial stromal cells (HESCs) were placed in culture and subjected to decidualization in vitro, in response to a hormone mixture containing E, P, and 8-bromo-cAMP as described previously (45–47). Examining HIF1α and HIF2α expression during in vitro decidualization, we noted distinct nuclear staining of HIF2α but not of HIF1α in HESCs with onset of decidualization (Fig. 7A). Attenuation of *HIF2α* by siRNA (Fig. 7B) led to a marked decline
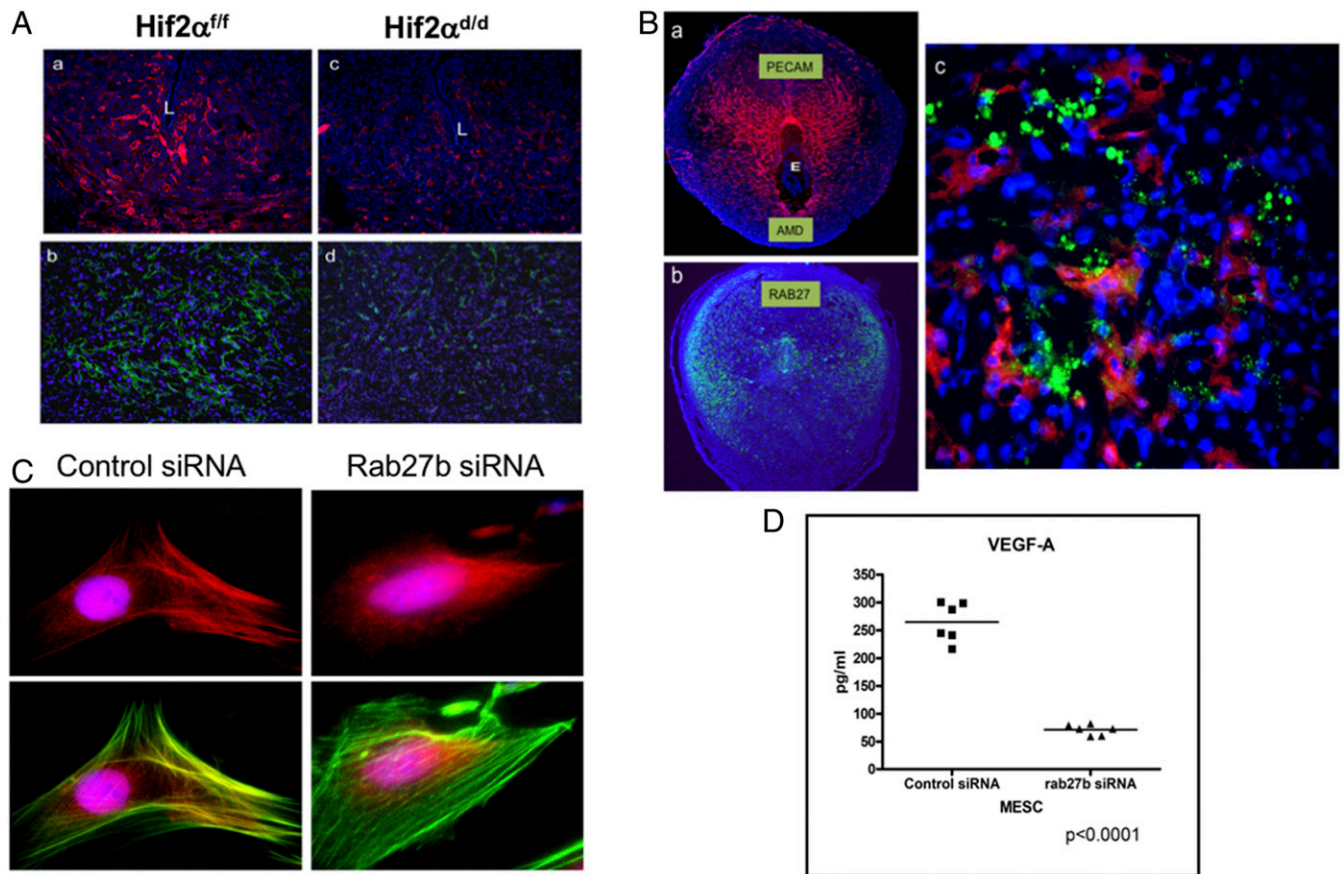
Bhurke et al.

www.manaraa.com

Fig. 6. Endometrial stromal angiogenesis is affected in *Hif2α^d/d* mice. (*A, Upper*) Uterine sections from *Hif2α^f/f* (*a*) and *Hif2α^d/d* (*c*) mice on day 6 of pregnancy were subjected to IF using PECAM (red) antibody. *n* = 4 mice were examined for each genotype. (*A, Lower*) Ovariectomized *Hif2α^f/f* (*b*) and *Hif2α^d/d* (*d*) mice were subjected to experimentally induced decidualization, as described in *Materials and Methods*. The uterine sections were subjected to IF using an antibody specific for PECAM. *n* = 3 mice were examined for each genotype. (*B*) Uterine sections on day 8 of pregnancy were subjected to IF using PECAM (*a*) and RAB27B (*b*) antibodies. *c* shows colocalization of PECAM and RAB27B in the uterus on day 8 of pregnancy. *n* = 3 mice were examined. (*C*) MESCs transfected with a scrambled siRNA (*Left*) and *Rab27b*-specific siRNA (*Right*) were fixed and subjected to IF using VEGFA antibody (*Upper*). *Lower* shows staining with VEGFA antibody and phalloidin. Data were repeated with three separate samples and for each sample 35 to 50 cells were examined over multiple fields. (*D*) Conditioned media from MESCs transfected with a scrambled siRNA and *Rab27b*-specific siRNA were analyzed for VEGFA using ELISA. Data represent mean ± SEM from three separate samples.

in levels of MMP-9 or VEGFA in the conditioned media (Fig. 7*C*), indicating that HIF2α regulates the secretory pathway in HESCs. HIF2α siRNA had no effect on HIF1α mRNA (Fig. 7 *B, Right*)

We also investigated the involvement of Rab27b in trafficking of MMP-9 and VEGFA secretory granules in HESCs. These stromal cells were transfected with siRNA targeted specifically to the mRNA of RAB27B; in control experiments, cells were transfected with a scrambled siRNA. HESCs treated with a siRNA targeted to *RAB27B* mRNA efficiently suppressed the level of its cognate mRNA but did not significantly affect the levels of *RAB27A*, *HIF2α*, *HIF1α*, *MMP-9*, or *VEGF* mRNAs (*SI Appendix*, Fig. S7). In HESCs transfected with control siRNA, CD63-positive secretory granules were distributed throughout the cell (Fig. 8 *A, Left*). By contrast, HESCs transfected with *RAB27B* siRNA showed CD63-positive secretory granules localized close to the nucleus (Fig. 8 *A, Right*). Consistent with these observations we found that the MMP-9 and VEGFA levels were significantly attenuated in the conditioned media of cultured HESCs transfected with *RAB27B* siRNAs compared to cells treated with control siRNAs (Fig. 8*B*). Collectively, our results support the notion that RAB27B functioning downstream of HIF2α regulates trafficking of MMP-9 and VEGF in mouse and human endometrial stromal cells.

Discussion

During early pregnancy, E acts in concert with P to orchestrate changes in the uterine epithelium, rendering it competent for embryo attachment and implantation (2, 12). As the uterine epithelium becomes receptive to interacting with an incoming embryo, the underlying stromal cells begin to proliferate, creating a hypoxic uterine environment during early pregnancy (48–50). In many mammalian species, including humans, the oxygen concentration in the uterine environment during implantation ranges from 1 to 5% (pO2 0.5 to 30 mmHg) (51). While it has long been known that the maternal environment during implantation is hypoxic (15, 16), the mechanisms of maternal adaptation to hypoxia during implantation have remained unclear.

HIFs serve as critical regulators of a tissue's response to changes in oxygen levels (13). While HIF1α is expressed ubiquitously, HIF2α is expressed in a tissue-restricted manner (13). HIF1α or HIF2α forms a complex with HIF1β/ARNT and the resulting heterodimer binds to target genes to regulate adaptive transcriptional responses to hypoxia (13). Here we report that, during implantation in mice and women, decidualizing hormones induce expression of HIF2α in the stromal cells. Ablation of HIF2α from murine endometrial stroma prevents embryo invasion, leading to implantation failure and infertility. Interestingly, HIF2α is also detectable in the human endometrial stroma during the first 10 wk
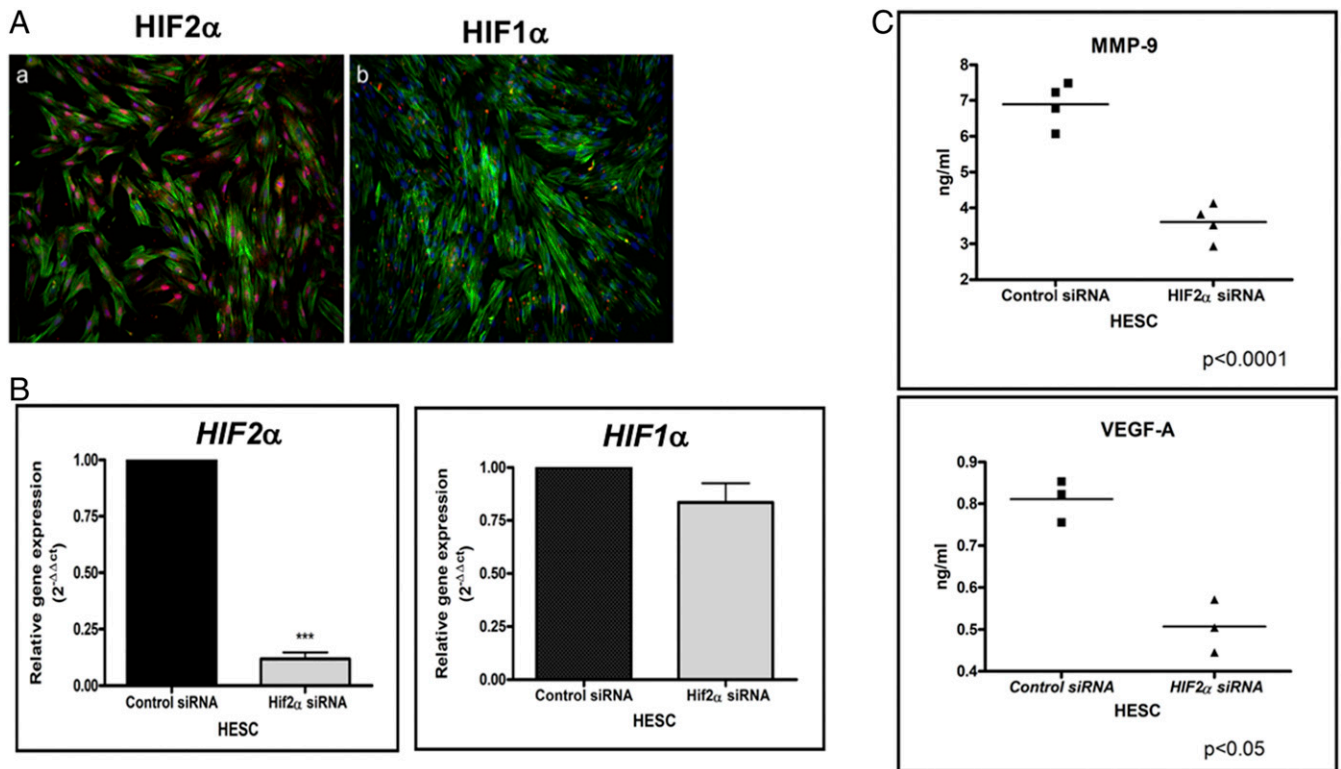
Fig. 7. HIF2α is induced in HESCs during stromal cell differentiation. (*A*) Immunocytochemical (ICC) analysis of HIF2α (*a*) and HIF1α (*b*) in HESCs on day 4 of culture under hypoxic conditions (3% O$_2$); HIF2α protein (red), actin (green). (*B*) HESCs were transfected with a *HIF2α*-specific siRNA and scrambled siRNA for controls. Cells were lysed to isolate total RNA and real-time PCR was performed to determine levels of *HIF2α* and *HIF1α*. (*C*) Conditioned media from HESCs transfected with a scrambled siRNA and *HIF2α*-specific siRNA were analyzed for MMP and VEGFA using ELISA. Data represent mean ± SEM from three separate samples.

of pregnancy when oxygen tension is 1 to 2%, which raises the possibility that HIF2α plays a critical and conserved function in rodents and humans (52–54).

Previous studies have suggested that HIF1α expression in uterine epithelium is likely to affect vascular permeability at implantation sites via local production of VEGF (22). Interestingly, pregnant Hif2α-ablated uteri, which retained epithelial expression of HIF1α, exhibited no alteration in vascular permeability at the sites of blastocyst apposition. However, despite close apposition and attachment of the blastocysts to the luminal epithelium, mice lacking uterine Hif2α displayed implantation failure and bore no offspring. These observations indicate that HIF1α and HIF2α have non-redundant roles in embryo implantation during early pregnancy.

Following attachment of the embryo to the uterine wall, structural remodeling disrupts the integrity of the luminal epithelium, enabling an embryo to breach the epithelium, disrupt the basement membrane, and invade the underlying stroma. Our studies show that, in mice with ablation of stromal Hif2α, epithelial remodeling—including degradation of the basement membrane and disruption of the epithelial cell–cell junctions—fails to occur. Previous studies have shown that MMPs such as *-2* and *Mmp-9* are expressed in the uterus at the time of implantation. MMPs are known to be responsible for remodeling extracellular matrix, especially degrading the basement membrane (26–31). In addition, some MMPs such as MMP-9 have been shown to disrupt cell–cell junctional complexes (55); and, in chondrocytes, HIF2α has been reported to regulate MMP-9 expression (33). Our results show that HIF2α does not affect MMP-9 gene expression in uterine cells but it does stimulate protein secretion. Interestingly, our previous study showed that E signaling via ESR1 regulates the expression of Fos-related antigen 1 (FRA-1), a member of the Fos family of transcription

factors, which in turn promotes the expression of MMP-9 in differentiating uterine stromal cells (56). Taken together, it appears that E induces expression of FRA-1 and HIF2α in stromal cells at the onset of implantation; and while FRA-1 regulates MMP-9 expression, HIF2α controls the trafficking pathway that regulate MMP-9 secretion.

Our studies revealed that RAB27B, a member of the RAB family GTPases, is a unique target of HIF2α. RABs mediate various protein trafficking events (57, 58). All cells have constitutive secretory vesicles, which carry newly synthesized proteins directly from the Golgi complex to the cell surface. However, certain secretory cells divert classes of secretory proteins away from the constitutive pathway into a specialized class of secretory vesicles: the secretory granules. These are small subcellular membrane-surrounded vesicles that form from the Golgi apparatus and contain densely packed proteins destined for secretion. Secretory granules move toward the periphery of a cell where, upon stimulation, their membranes fuse with the cell membrane and their protein load is exteriorized. RAB27B is specifically involved in the controlled release of secretory granules, including platelet dense granules and pancreatic acinar granules, in response to appropriate physiological signals (34, 35, 59); and down-regulation of RAB27B in human glioblastoma cells decreases the amount of active MMP-9 in the extracellular matrix (60). Decidual cells in rodents and humans are known to possess dense secretory granules (61), so it is conceivable that the Hif2α-Rab27b pathway mediates regulated exocytosis of these granules to control endometrial function in a stage-specific manner.

Our study demonstrates that HIF2α directly regulates the expression of RAB27B, which mediates movement of secretory granules containing MMP-9 toward the cell periphery. Interestingly,
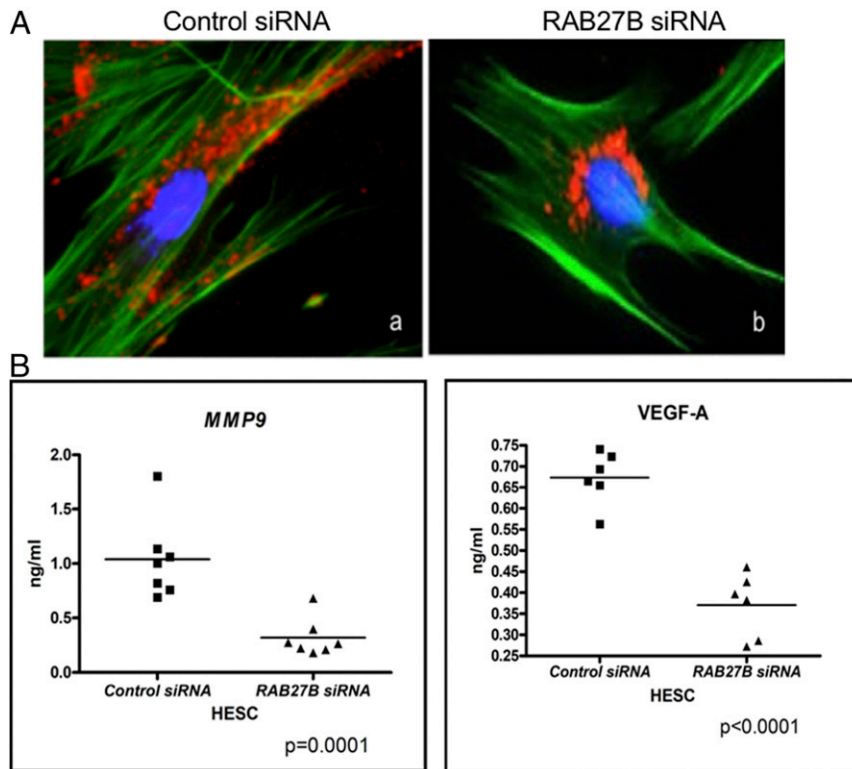
Bhurke et al.

www.manaraa.com

Fig. 8. RAB27B-mediated granular secretion in HESCs. (*A*) HESCs transfected with a scrambled siRNA (*a*) and *RAB27b*-specific siRNA (*b*) were fixed and subjected to IF using CD63 (red) antibody. (*B*) Conditioned media from HESCs transfected with a scrambled siRNA and *RAB27B*-specific siRNA were analyzed for MMP-9 (*Left*) and VEGFA (*Right*) using ELISA. Data represent mean ± SEM from three separate samples.

these secretory granules also transport CD63, a transmembrane glycoprotein. Recent studies have shown that the N-terminal region of CD63 can interact with certain MMPs to facilitate intracellular trafficking of MMPs (62). We speculate that CD63 is involved either in sorting these MMPs into the secretory granules or in degranulation (exocytosis) of the secretory vesicles containing MMP-9. Further studies are needed to gain a comprehensive understanding of the secretory pathways operating in the decidual cells during early pregnancy.

As the embryo breaches the luminal epithelium and invades the stroma, the stromal cells undergo a dramatic transformation to form a specialized tissue known as the decidua. During this process, termed decidualization, fibroblastic stromal cells proliferate and then differentiate into secretory decidual cells that support embryo growth and survival until placentation ensues (1–4). As the decidua forms around the implanted embryo, uterine endothelial cells proliferate to create an extensive vascular network that is embedded in the decidua and critical for embryo development (5, 6). Our studies revealed that differentiation of stromal cells to form decidual cells, as indicated by expression of a subset of differentiation markers, is not affected by the loss of HIF2α. A recent study reported that loss of uterine HIF2α causes implantation failure by affecting decidualization and degradation of the embryo on day 8 of pregnancy (63). While we observed no impact of HIF2α on decidualization, we did note a drastic decrease on day 8 in the development of the uterine vascular network that supports embryonic growth. Interestingly, HIF2α does not regulate expression of VEGFA by decidual cells but instead controls its secretion. Stromal cells in proximity to the endothelial cells that proliferate to form the angiogenic network express RAB27B, which then promotes granular secretion of VEGFA to regulate stromal angiogenesis in a stage-specific manner during early pregnancy.

An important finding of this study is that in rodents and humans, the HIF2α-RAB27B pathway mediating secretion of MMP-9 and VEGFA is conserved. Notably, the levels of MMP-9 and VEGFA declined markedly upon attenuation of *HIF2α* and *RAB27B* in HESCs. In summary, this study demonstrates that a hypoxic environment is essential for secretion of proteins that facilitates embryo invasion and later angiogenesis during early pregnancy. Interestingly, a genome-wide allelic differentiation scan comparing indigenous highlanders of the Tibetan Plateau (3,200 to 3,500 m) with a closely related lowland Han population, revealed a genome-wide significant divergence across eight single-nucleotide polymorphisms (SNPs) located near *HIF2α*. The SNPs identified in *HIF2α* are associated with lower rates of pregnancy loss in indigenous Tibetan highlanders as compared to the Han (64). Following this report, a more recent study identified a mutational hot spot in *HIF2α* that is associated with recurrent pregnancy loss (65). While no reports to date link loss of MMP-9 to human infertility, a previous study indicated that in women with recurrent miscarriage, endometrial VEGFA expression is reduced (66). More studies are needed to determine whether an impaired HIF2α-RAB27B pathway is involved in affecting establishment of pregnancy and causing miscarriage in the human.

Materials and Methods

Animals. Mice were maintained in the designated animal care facility at the College of Veterinary Medicine of the University of Illinois at Urbana–Champaign, according to the institutional guidelines for the care and use of laboratory animals. The Institutional Animal Use and Care Committee at the University of Illinois at Urbana–Champaign approved all procedures involving animal care, killing, and tissue collection. Conditional *Hif2α*-null mice (*Hif2α^d/d^*) were generated by crossing mice harboring a floxed *Hif2α* gene (The Jackson Laboratory) with *Pgr-Cre* knockin mice, as described previously (47). Francesco J. DeMayo, National Institute of Environmental Health Sciences, Durham, NC,

Bhurke et al.

www.manaraa.com

and John P. Lydon, Baylor College of Medicine, Houston, TX, provided the *Pgr-Cre* knockin mice (67).

Chemicals, Reagents, and Antibodies. As reported previously (47), progesterone (P), 17β-estradiol (E), naphthol AS-MX phosphate, Fast Blue RR (4-benzoylamino- 2,5-dimethoxyaniline diazonium), collagenase, pancreatin, dimethyl sulfoxide (DMSO), 8-bromoadenosine 3′,5′-cyclic monophosphate salt, and Trypan blue were purchased from Sigma. Fetal bovine serum was purchased from Fisher Scientific. Fluoromount-G with DAPI was purchased from eBiosciences.

Primary antibodies including hypoxia-inducible factor 2 alpha (Hif2α, 1:200, Novus, 122), hypoxia-inducible factor 1 alpha (Hif1α, 1:200, Santa Cruz Biotechnology, sc-10790), Ras-related in brain 27B (RAB27B, 1:200, Santa Cruz Biotechnology, sc-22993), matrix metalloproteases 9 (MMP9, 1:200 Abcam, ab38898), matrix metalloproteases 2 (MMP2, 1:200 Life Technology, 436000), vascular endothelial growth factor A (VEGFA, 1:100, Santa Cruz Biotechnology, sc-152), cytokeratin 8 (KRT8, 1:50, Developmental Studies Hybridoma Bank, TROMA-I), platelet/endothelial cell adhesion molecule 1 (PECAM1/CD31, 1:500, BD Pharmigen, 557355), E-cadherin (1:200, Santa Cruz Biotechnology, sc-7870), and CD63 (CD63, 1:200, ab193349) were employed for immunohistochemical analysis of uterine sections or endometrial stromal cells as described previously in ref. 47. The secondary antibodies that were used for analyses include rhodamine or Cy3 donkey anti-rabbit, Cy3 donkey anti-mouse, 488 donkey anti-mouse, 488 donkey anti-goat, and Cy3 donkey anti-rat. For immunocytochemistry, F-actin filaments were stained using phalloidin conjugated to Alexa 488.

The siRNA oligos against human *EPAS1* (EntrezGene:2034) were purchased from Dharmacon (L-004814-00-0020). The siRNA oligos targeting human *RAB27B* (EntrezGene:5874), purchased from Dharmacon (L-004228-00-0020), were used to silence the expression of *RAB27B* in the human endometrial stromal cells. The siRNA oligos targeting mouse *RAB27B* (EntrezGene:80718), purchased from Dharmacon (L-050808-01-0020) were used to silence the expression of *RAB27B* in the mouse endometrial stromal cells. The siRNA oligos used for silencing each of the above-mentioned genes consisted of a mixture of four siRNA provided as a single reagent (SMARTpool). Nontargeting siRNA oligos used as control were purchased from Dharmacon (D-001810-01-05).

Full details of fertility assessments, delayed implantation, experimentally induced decidualization, primary mouse and human endometrial stromal cultures, immunofluorescence analysis, real-time qPCR, chromatin immuno-precipitation, siRNA transfections, microarray analysis, ELISA, and statistical analyses can be found in *SI Appendix, SI Materials and Methods*.

Data Availability. Microarray data reported in this paper have been deposited in the Gene Expression Omnibus (GEO) database (accession no. GSE146650).

1. C. Y. Ramathal, I. C. Bagchi, R. N. Taylor, M. K. Bagchi, Endometrial decidualization: Of mice and men. *Semin. Reprod. Med.* **28**, 17–26 (2010).
2. S. Pawar, A. M. Hantak, I. C. Bagchi, M. K. Bagchi, Minireview: Steroid-regulated paracrine mechanisms controlling implantation. *Mol. Endocrinol.* **28**, 1408–1422 (2014).
3. Y. M. Vasquez, F. J. DeMayo, Role of nuclear receptors in blastocyst implantation. *Semin. Cell Dev. Biol.* **24**, 724–735 (2013).
4. S. Zhang et al., Physiological and molecular determinants of embryo implantation. *Mol. Aspects Med.* **34**, 939–980 (2013).
5. A. M. Hantak, I. C. Bagchi, M. K. Bagchi, Role of uterine stromal-epithelial crosstalk in embryo implantation. *Int. J. Dev. Biol.* **58**, 139–146 (2014).
6. K. Red-Horse et al., Trophoblast differentiation during embryo implantation and formation of the maternal-fetal interface. *J. Clin. Invest.* **114**, 744–754 (2004).
7. A. M. Sharkey, S. K. Smith, The endometrium as a cause of implantation failure. *Best Pract. Res. Clin. Obstet. Gynaecol.* **17**, 289–307 (2003).
8. E. R. Norwitz, Defective implantation and placentation: Laying the blueprint for pregnancy complications. *Reprod. Biomed. Online* **13**, 591–599 (2006).
9. E. Jauniaux, R. H. Van Oppenraaij, G. J. Burton, Obstetric outcome after early placental complications. *Curr. Opin. Obstet. Gynecol.* **22**, 452–457 (2010).
10. J. C. Cross, Z. Werb, S. J. Fisher, Implantation and the placenta: Key pieces of the development puzzle. *Science* **266**, 1508–1518 (1994).
11. H. Wang, S. K. Dey, Roadmap to embryo implantation: Clues from mouse models. *Nat. Rev. Genet.* **7**, 185–199 (2006).
12. J. Cha, X. Sun, S. K. Dey, Mechanisms of implantation: Strategies for successful pregnancy. *Nat. Med.* **18**, 1754–1767 (2012).
13. B. Keith, R. S. Johnson, M. C. Simon, HIF1α and HIF2α: Sibling rivalry in hypoxic tumour growth and progression. *Nat. Rev. Cancer* **12**, 9–22 (2011).
14. T. Daikoku et al., Expression of hypoxia-inducible factors in the peri-implantation mouse uterus is regulated in a cell-specific and ovarian steroid hormone-dependent manner. Evidence for differential function of HIFs during early pregnancy. *J. Biol. Chem.* **278**, 7683–7691 (2003).
15. D. M. Adelman, M. Gertsenstein, A. Nagy, M. C. Simon, E. Maltepe, Placental cell fates are regulated in vivo by HIF-mediated hypoxia responses. *Genes Dev.* **14**, 3191–3203 (2000).
16. G. X. Rosario, T. Konno, M. J. Soares, Maternal hypoxia activates endovascular trophoblast cell invasion. *Dev. Biol.* **314**, 362–375 (2008).
17. M. B. Renfree, G. Shaw, Diapause. *Annu. Rev. Physiol.* **62**, 353–375 (2000).
18. J. Van Blerkom, D. J. Chavez, H. Bell, Molecular and cellular aspects of facultative delayed implantation in the mouse. *Ciba Found. Symp.*, 141–172 (1978).
19. K. Yoshinaga, C. E. Adams, Delayed implantation in the spayed, progesterone treated adult mouse. *J. Reprod. Fertil.* **12**, 593–595 (1966).
20. S. Nallasamy, Q. Li, M. K. Bagchi, I. C. Bagchi, Msx homeobox genes critically regulate embryo implantation by controlling paracrine signaling between uterine stroma and epithelium. *PLoS Genet.* **8**, e1002500 (2012).
21. Q. Li et al., The antiproliferative action of progesterone in uterine epithelium is mediated by Hand2. *Science* **331**, 912–916 (2011).
22. A. A. Kazi, R. D. Koos, Estrogen-induced activation of hypoxia-inducible factor-1alpha, vascular endothelial growth factor expression, and edema in the uterus are mediated by the phosphatidylinositol 3-kinase/Akt pathway. *Endocrinology* **148**, 2363–2374 (2007).
23. T. N. Blankenship, R. L. Given, Loss of laminin and type IV collagen in uterine luminal epithelial basement membranes during blastocyst implantation in the mouse. *Anat. Rec.* **243**, 27–36 (1995).
24. S. Pawar et al., STAT3 regulates uterine epithelial remodeling and epithelial-stromal crosstalk during implantation. *Mol. Endocrinol.* **27**, 1996–2012 (2013).
25. M. Thie, P. Fuchs, H. W. Denker, Epithelial cell polarity and embryo implantation in mammals. *Int. J. Dev. Biol.* **40**, 389–393 (1996).
26. L. A. Salamonsen, D. E. Woolley, Matrix metalloproteinases in normal menstruation. *Hum. Reprod.* **11** (suppl. 2), 124–133 (1996).
27. L. A. Salamonsen, Role of proteases in implantation. *Rev. Reprod.* **4**, 11–22 (1999).
28. B. M. Bany, M. B. Harvey, G. A. Schultz, Expression of matrix metalloproteinases 2 and 9 in the mouse uterus during implantation and oil-induced decidualization. *J. Reprod. Fertil.* **120**, 125–134 (2000).
29. J. R. Hinchliffe, A. M. El-Shershaby, Epithelial cell death in the oil-induced decidual reaction of the pseudopregnant mouse: An ultrastructural study. *J. Reprod. Fertil.* **45**, 463–468 (1975).
30. C. M. Alexander et al., Expression and function of matrix metalloproteinases and their inhibitors at the maternal-embryonic boundary during mouse embryo implantation. *Development* **122**, 1723–1736 (1996).
31. A. Weiss, S. Goldman, E. Shalev, The matrix metalloproteinases (MMPS) in the decidua and fetal membranes. *Front. Biosci.* **12**, 649–659 (2007).
32. G. Murphy et al., Mechanisms for pro matrix metalloproteinase activation. *APMIS* **107**, 38–44 (1999).
33. S. Yang et al., Hypoxia-inducible factor-2alpha is a catabolic regulator of osteoarthritic cartilage destruction. *Nat. Med.* **16**, 687–693 (2010).
34. H. Gomi, K. Mori, S. Itohara, T. Izumi, Rab27b is expressed in a wide range of exocytic cells and involved in the delivery of secretory granules near the plasma membrane. *Mol. Biol. Cell* **18**, 4377–4386 (2007).
35. T. Tolmachova, M. Abrink, C. E. Futter, K. S. Authi, M. C. Seabra, Rab27b regulates number and secretion of platelet dense granules. *Proc. Natl. Acad. Sci. U.S.A.* **104**, 5872–5877 (2007).
36. L. Källquist et al., The tetraspanin CD63 is involved in granule targeting of neutrophil elastase. *Blood* **112**, 3444–3454 (2008).
37. L. A. Carmo et al., CD63 is tightly associated with intracellular, secretory events chaperoning piecemeal degranulation and compound exocytosis in human eosinophils. *J. Leukoc. Biol.* **100**, 391–401 (2016).
38. K. E. Orwig, G. Dai, C. A. Rasmussen, M. J. Soares, Decidual/trophoblast prolactin-related protein: Characterization of gene structure and cell-specific expression. *Endocrinology* **138**, 2491–2500 (1997).
39. M. J. Soares, H. Müller, K. E. Orwig, T. J. Peters, G. Dai, The uteroplacental prolactin family and pregnancy. *Biol. Reprod.* **58**, 273–284 (1998).
40. C. A. Finn, J. R. Hinchliffe, Reaction of the mouse uterus during implantation and deciduoma formation as demonstrated by changes in the distribution of alkaline phosphatase. *J. Reprod. Fertil.* **8**, 331–338 (1964).
41. Q. Li et al., Bone morphogenetic protein 2 functions via a conserved signaling pathway involving Wnt4 to regulate uterine decidualization in the mouse and the human. *J. Biol. Chem.* **282**, 31725–31732 (2007).
42. M. J. Laws et al., Gap junction communication between uterine stromal cells plays a critical role in pregnancy-associated neovascularization and embryo survival. *Development* **135**, 2659–2668 (2008).
43. K. Y. Lee et al., Bmp2 is critical for the murine uterine decidual response. *Mol. Cell. Biol.* **27**, 5468–5478 (2007).
44. J. P. Lydon et al., Mice lacking progesterone receptor exhibit pleiotropic reproductive abnormalities. *Genes Dev.* **9**, 2266–2278 (1995).
45. B. Tang, S. Guller, E. Gurpide, Cyclic adenosine 3′,5′-monophosphate induces prolactin expression in stromal cells isolated from human proliferative endometrium. *Endocrinology* **133**, 2197–2203 (1993).
46. I. P. Ryan, E. D. Schriock, R. N. Taylor, Isolation, characterization, and comparison of human endometrial and endometriosis cells in vitro. *J. Clin. Endocrinol. Metab.* **78**, 642–649 (1994).

Bhurke et al.

PHYSIOLOGY

47. J. Davila *et al.*, Rac1 regulates endometrial secretory function to control placental development. *PLoS Genet.* **11**, e1005458 (2015).

48. P. Quinn, G. M. Harlow, The effect of oxygen on the development of preimplantation mouse embryos in vitro. *J. Exp. Zool.* **206**, 73–80 (1978).

49. J. A. Mitchell, J. M. Yochim, Measurement of intrauterine oxygen tension in the rat and its regulation by ovarian steroid hormones. *Endocrinology* **83**, 691–700 (1968).

50. A. J. Harvey, The role of oxygen in ruminant preimplantation embryo development and metabolism. *Anim. Reprod. Sci.* **98**, 113–128 (2007).

51. K. Okazaki, E. Maltepe, Oxygen, epigenetics and stem cell fate. *Regen. Med.* **1**, 71–83 (2006).

52. F. Rodesch, P. Simon, C. Donner, E. Jauniaux, Oxygen measurements in endometrial and trophoblastic tissues during early pregnancy. *Obstet. Gynecol.* **80**, 283–285 (1992).

53. J. L. James, P. R. Stone, L. W. Chamley, The effects of oxygen concentration and gestational age on extravillous trophoblast outgrowth in a human first trimester villous explant model. *Hum. Reprod.* **21**, 2699–2705 (2006).

54. J. A. Maybin *et al.*, Hypoxia and hypoxia inducible factor-1α are required for normal endometrial repair during menstruation. *Nat. Commun.* **9**, 295 (2018).

55. J. Symowicz *et al.*, Engagement of collagen-binding integrins promotes matrix metalloproteinase-9-dependent E-cadherin ectodomain shedding in ovarian carcinoma cells. *Cancer Res.* **67**, 2030–2039 (2007).

56. A. Das *et al.*, Estrogen-induced expression of Fos-related antigen 1 (FRA-1) regulates uterine stromal differentiation and remodeling. *J. Biol. Chem.* **287**, 19622–19630 (2012).

57. T. Bhuin, J. K. Roy, Rab proteins: The key regulators of intracellular vesicle transport. *Exp. Cell Res.* **328**, 1–19 (2014).

58. F. A. Barr, Review series: Rab GTPases and membrane identity: Causal or inconsequential? *J. Cell Biol.* **202**, 191–199 (2013).

59. R. D. Burgoyne, A. Morgan, Secretory granule exocytosis. *Physiol. Rev.* **83**, 581–632 (2003).

60. H. Wang *et al.*, Hypomethylated Rab27b is a progression-associated prognostic biomarker of glioma regulating MMP-9 to promote invasion. *Oncol. Rep.* **34**, 1503–1509 (2015).

61. B. Lane, W. Oxberry, J. Mazella, L. Tseng, Decidualization of human endometrial stromal cells in vitro: Effects of progestin and relaxin on the ultrastructure and production of decidual secretory proteins. *Hum. Reprod.* **9**, 259–266 (1994).

62. T. Takino *et al.*, Tetraspanin CD63 promotes targeting and lysosomal proteolysis of membrane-type 1 matrix metalloproteinase. *Biochem. Biophys. Res. Commun.* **304**, 160–166 (2003).

63. L. Matsumoto *et al.*, HIF2α in the uterine stroma permits embryo invasion and luminal epithelium detachment. *J. Clin. Invest.* **128**, 3186–3197 (2018).

64. C. M. Beall *et al.*, Natural selection on EPAS1 (HIF2alpha) associated with low hemoglobin concentration in Tibetan highlanders. *Proc. Natl. Acad. Sci. U.S.A.* **107**, 11459–11464 (2010).

65. P. Quintero-Ronderos *et al.*, Novel genes and mutations in patients affected by recurrent pregnancy loss. *PLoS One* **12**, e0186149 (2017).

66. P. Vuorela, O. Carpén, M. Tulppala, E. Halmesmäki, VEGF, its receptors and the tie receptors in recurrent miscarriage. *Mol. Hum. Reprod.* **6**, 276–282 (2000).

67. S. M. Soyal *et al.*, Cre-mediated recombination in cell lineages that express the progesterone receptor. *Genesis* **41**, 58–66 (2005).

www.manaraa.com